1-1-2002

Three-Dimensional Structure of the Complexin/SNARE Complex

Xiaocheng Chen
University of Texas Southwestern Medical Center at Dallas

Diana R. Tomchick
University of Texas Southwestern Medical Center at Dallas

Evgueni Kovriguine
Marquette University, evgueni.kovriguine@marquette.edu

Demet Araç
University of Texas Southwestern Medical Center at Dallas

Mischa Machius
University of Texas Southwestern Medical Center at Dallas

See next page for additional authors

Accepted version. *Neuron*, Vol. 33, No. 3 (January 2002): 397-409. DOI:

Authors
Xiaocheng Chen, Diana R. Tomchick, Evgueni Kovriguine, Demet Araç, Mischa Machius, Thomas C. Südhof, and Josep Rizo

Neuron, Vol. 33, No. 3 (2002): 397-409. DOI.

Three-Dimensional Structure of the Complexin/SNARE Complex

Xiaocheng Chen
Department of Biochemistry, Dallas, TX 75390 USA
Department of Pharmacology, Dallas, TX 75390 USA
Diana R. Tomchick
Department of Biochemistry, Dallas, TX 75390 USA
Evguenii Kovrigin
Department of Chemistry, Marquette University, Milwaukee, WI
Department of Biochemistry, Dallas, TX 75390 USA
Department of Pharmacology, Dallas, TX 75390 USA
Demet Araç
Department of Biochemistry, Dallas, TX 75390 USA
Department of Pharmacology, Dallas, TX 75390 USA
Mischa Machius
Department of Biochemistry, Dallas, TX 75390 USA
Thomas C. Südhof
Department of Molecular Genetics, Dallas, TX 75390 USA
Center for Basic Neuroscience, Dallas, TX 75390 USA
Howard Hughes Medical Institute, University of Texas Southwestern Medical Center, 5323 Harry Hines Boulevard, Dallas, TX 75390 USA
Josep Rizo
Department of Biochemistry, Dallas, TX 75390 USA
Department of Pharmacology, Dallas, TX 75390 USA

Abstract

During neurotransmitter release, the neuronal SNARE proteins synaptobrevin/VAMP, syntaxin, and SNAP-25 form a four-helix bundle, the SNARE complex, that pulls the synaptic vesicle and plasma membranes together possibly causing membrane fusion. Complexin binds tightly to the SNARE complex and is essential for efficient Ca^{2+}-evoked neurotransmitter release. A combined X-ray and TROSY-based NMR study now reveals the atomic structure of the complexin/SNARE complex. Complexin binds in an antiparallel α-helical conformation to the groove between the synaptobrevin and syntaxin helices. This interaction stabilizes the interface between these two helices, which bears the repulsive forces between the apposed membranes. These results suggest that complexin stabilizes the fully assembled SNARE complex as a key step that enables the exquisitely high speed of Ca^{2+}-evoked neurotransmitter release.

Introduction

Neurotransmitters are released by synaptic vesicle exocytosis in a very fast (<1 ms) and tightly regulated reaction. The speed of exocytosis is critical for neural function and relies on a cascade of protein-protein interactions that mediate docking of syntaptic vesicles to the plasma membrane, a priming step(s) that prepares the vesicles for release and the actual release upon Ca^{2+} influx (Südhof, 1995). Critical among these interactions are those involving the synaptic vesicle protein synaptobrevin/VAMP and the plasma membrane proteins syntaxin and SNAP-25, which belong to the SNARE protein family (for soluble N-ethylmaleimide sensitive factor attachments receptors) Jahn and Südhof 1999, Lin and Scheller 2000. These proteins form a tight complex via sequences called SNARE motifs Söllner et al. 1993, Hayashi et al. 1994. This complex is known as the SNARE or core complex and consists of a bundle of four parallel α helices (Sutton et al., 1998). Since the SNARE motifs of synaptobrevin and syntaxin are adjacent to their C-terminal transmembrane regions, the free energy of SNARE complex formation may be used to overcome the energy barrier required to bring the synaptic vesicle and plasma membranes together, perhaps causing membrane fusion (Hanson et al., 1997). The observation that homologs of the neuronal SNAREs are required for membrane traffic in all cellular compartments (Pelham, 1999) suggests that similar SNARE complexes mediate all types of intracellular membrane fusion.

Whereas the above results have led to a working model of SNARE function, it is still under debate whether SNARE complex assembly causes or precedes membrane fusion (see Weber et al. 1998, Ungermann et al. 1998, Schoch et al. 2001), and the mechanisms of the different steps that lead to neurotransmitter release remain unclear. In order to unravel these mechanisms, it is critical to determine the roles of additional proteins that are involved in exocytosis and that may regulate assembly or disassembly of the SNARE complex, which may in turn help to further understand SNARE function. Particularly interesting among these proteins are the complexins (also known as synaphins; McMahon et al. 1995, Takahashi et al. 1995). Complexins constitute a small family of soluble neuronal proteins that include two closely related isoforms (complexins 1 and 2) and exhibit a number of unique properties. Both isoforms are small (15–16 kDa) and highly charged, and their sequences are remarkably conserved through evolution. Complexins colocalize with the SNAREs and bind tightly to the SNARE complex McMahon et al. 1995, Ishizuka et al. 1995. Nuclear magnetic resonance (NMR) analysis revealed that complexins lack a tertiary structure, yet they contain an α-helical region in the middle of their sequence (Pabst et al., 2000). This helical region is responsible for binding to the SNARE complex, which probably involves the syntaxin and synaptobrevin SNARE motifs McMahon et al. 1995, Pabst et al. 2000. The functional importance of complexins has been demonstrated by the lethal phenotype caused by double knockout of the complexin 1 and 2 genes in mice (Reim et al., 2001). This phenotype is associated with a selective decrease in the efficiency of fast Ca^{2+}-triggered release, whereas release by hypertonic sucrose is unaffected. Additional interest in complexins has arisen from the observation that complexin mRNA levels are decreased in some hippocampal subfields of patients with schizophrenia or bipolar disorder (Eastwood and Harrison, 2000) and that complexin 2 is progressively depleted in a mouse model of Huntington's disease (Morton and Edwardson, 2001). Hence,

understanding the function of complexins is not only important to elucidate how neurotransmitter release is regulated, but it may also provide clues on the etiology of grave human diseases.

Complexins have been suggested to induce oligomerization of SNARE complexes by reshuffling the two SNARE motifs of SNAP-25 into separate SNARE complexes (Tokumaru et al., 2001), but this model is inconsistent with the available biochemical data on complexin/SNARE interactions (Pabst et al., 2000), and SNAP-25-mediated oligomerization is not required for exocytosis in PC12 cells (Chen et al., 1999). On the other hand, the selective decrease in fast Ca^{2+}-evoked neurotransmitter release observed in the complexin double knockout mice, which suggests a role in a late step of exocytosis (Reim et al., 2001), is intriguing since complexins bind to the SNARE complex in a Ca^{2+}-independent manner. To gain further insights into how complexins function, we have studied the interaction of complexin 1 with the SNARE complex at atomic resolution using a combination of NMR spectroscopy and X-ray crystallography. Our results show that complexin binds in an antiparallel, α-helical conformation to the groove between the synaptobrevin and syntaxin SNARE motifs. Complexin binding does not alter the structure of the core complex but stabilizes the synaptobrevin/syntaxin interface. Since this interface bears the strong repulsive forces between the synaptic vesicle and plasma membranes, these results suggest a model whereby complexin stabilizes a primed state that involves full SNARE complex assembly and is critical for efficient Ca^{2+}-triggered neurotransmitter release.

Results

NMR Analysis of the Complexin/SNARE Complex

In previous NMR studies, the disappearance of the ^{1}H-^{15}N heteronuclear single quantum coherence (HSQC) cross-peaks from the central helical region of complexin upon addition of the SNARE complex indicated that this region is responsible for binding (Pabst et al., 2000). The disappearance of cross-peaks arose from the natural resonance broadening associated with formation of a larger protein complex and was compounded by the tendency of the SNARE complex to aggregate. To facilitate a more detailed analysis of this interaction by NMR spectroscopy, we took advantage of the observation that deletion of five residues at the C terminus of the syntaxin SNARE motif dramatically reduces the aggregation of the SNARE complex (Margittai et al., 2001). Thus, we prepared syntaxin, synaptobrevin, and SNAP-25 fragments corresponding to the minimal sequences involved in the SNARE complex (Sutton et al., 1998) with the exception that the syntaxin fragment was truncated at residue 253. Analysis by SDS-PAGE showed that stoichiometric amounts of these fragments assemble almost quantitatively into an SDS-resistant complex, and thermal melting experiments monitored by circular dichroism showed that this complex denatures above 90°C (data not shown), similarly to nontruncated versions of the SNARE complex (Fasshauer et al., 1997). In addition, this minimal SNARE complex bound stoichiometrically to a fragment spanning the complexin central helix (Cpx26-83), as determined by nondenaturing PAGE, and was found to remain monomeric by dynamic light scattering and one-dimensional NMR spectroscopy up to a concentration of 300 μM in the presence or absence of an equivalent amount of Cpx26-83 (data not shown).

Based on the above results, we initiated a more detailed characterization of the complexin/SNARE complex interaction by transverse-relaxation optimized spectroscopy (TROSY)-based NMR experiments (Pervushin et al., 1997), using different combinations of isotopically labeled and unlabeled samples of the minimal SNARE fragments and Cpx26-83. Similarly to ^{1}H-^{15}N HSQC spectra, ^{1}H-^{15}N TROSY-HSQC spectra can be considered like protein fingerprints that contain one cross-peak for each nonproline residue in the protein, and changes in the ^{1}H-^{15}N TROSY-HSQC spectrum of a ^{2}H,^{15}N-labeled protein(s) upon binding to an unlabeled protein(s) can be used to map the region of the labeled protein(s) involved in the interaction. In addition, the cross-peak dispersion observed in ^{1}H-^{15}N TROSY-HSQC spectra is indicative of the presence or absence of a well-defined tertiary or quaternary structure in a protein. Thus, the ^{1}H-^{15}N TROSY-HSQC spectrum of isolated ^{2}H,^{15}N-labeled Cpx26-83 (Figure 1A, black contours) exhibits poor chemical shift dispersion due to the absence of tertiary structure, as observed for full-length complexin (Pabst et al., 2000). Upon addition of the unlabeled minimal SNARE complex, we observed a striking dispersion of a subset of the complexin cross-peaks (Figure 1A, red contours), which were generally broader than less perturbed cross-peaks. This dispersion and broadening effects arise from the

formation of quaternary contacts between a specific region of Cpx26-83 and the SNARE complex. A practically superimposable spectrum was obtained when $^{2}H,^{15}N$-labeled Cpx26-83 was bound to a SNARE complex with a full syntaxin SNARE motif (Figure 1B), further demonstrating that complexin binding is not affected by the C-terminal truncation of the syntaxin SNARE motif (note that the more severe broadening observed in this spectrum is expected due to the tendency of the nontruncated SNARE complex to aggregate). Thus, all further analysis was performed using the minimal SNARE complex with the truncated syntaxin SNARE motif.

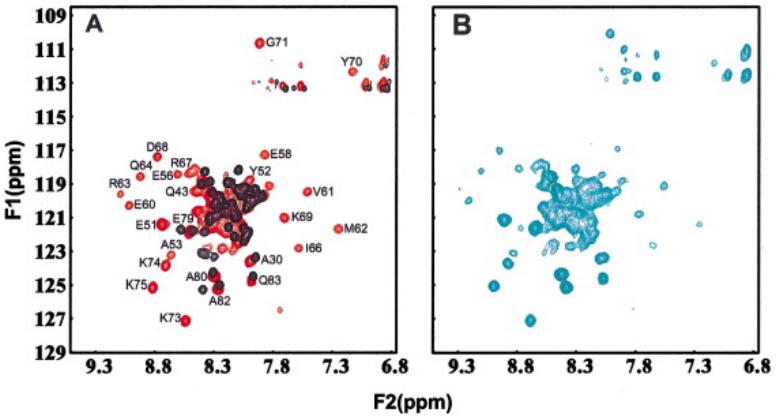

Figure 1. ^{1}H-^{15}N TROSY-HSQC Spectra Reveal the Region of Complexin that Binds to the SNARE Complex
(A) ^{1}H-^{15}N TROSY-HSQC spectra of $^{2}H,^{15}N$-labeled Cpx26-83 in isolation (black contours) or bound to the minimal SNARE complex containing the C-terminally truncated syntaxin SNARE motif (red contours). The assignments of the well-resolved backbone cross-peaks from the bound form are shown.
(B) ^{1}H-^{15}N TROSY-HSQC spectra of $^{2}H,^{15}N$-labeled Cpx26-83 bound to the SNARE complex formed with the full syntaxin SNARE motif.

Assignment of most of the backbone resonances of Cpx26-83 bound to the SNARE complex showed that the well-dispersed, broader ^{1}H-^{15}N TROSY-HSQC cross-peaks correspond primarily to the region encompassing residues 50–70 of complexin (Figure 1A), which, thus, constitutes the region directly involved in binding to the SNARE complex. The assignments also revealed Cα chemical shifts that are downfield shifted with respect to those of a random coil throughout most of the sequence (data not shown), indicating that Cpx26-83 binds to the SNARE complex in a largely α-helical conformation. Comparison of the chemical shifts of isolated complexin (Pabst et al., 2000) with those observed for Cpx26-83 bound to the SNARE complex (Figures 2A and 2B) showed that the largest chemical shift changes induced by the interaction occur in the binding region (residues 50–70). However, substantial chemical changes were observed beyond this region and included downfield shifts in the Cα carbons that reflect an increase in the population of α-helical conformation. These changes arise from stabilization of the helical conformation present in isolated complexin, which is stable in the N-terminal half of residues 26–83, but is only partially populated in the C-terminal half of this sequence (Pabst et al., 2000). Hence, this helix stabilization effect upon binding to the SNARE complex propagates beyond the binding region and results in widespread chemical shift changes. However, the chemical shifts of the 16 N-terminal residues of Cpx26-83 bound to the SNARE complex are remarkably similar to those observed in free complexin (Figures 2A and 2B). Thus, this region is clearly not involved in direct binding to the SNARE complex, but its high α-helical propensity may indirectly increase the affinity of the interaction by helping to nucleate an α-helical conformation in the more C-terminal residues that bind to the SNARE complex.

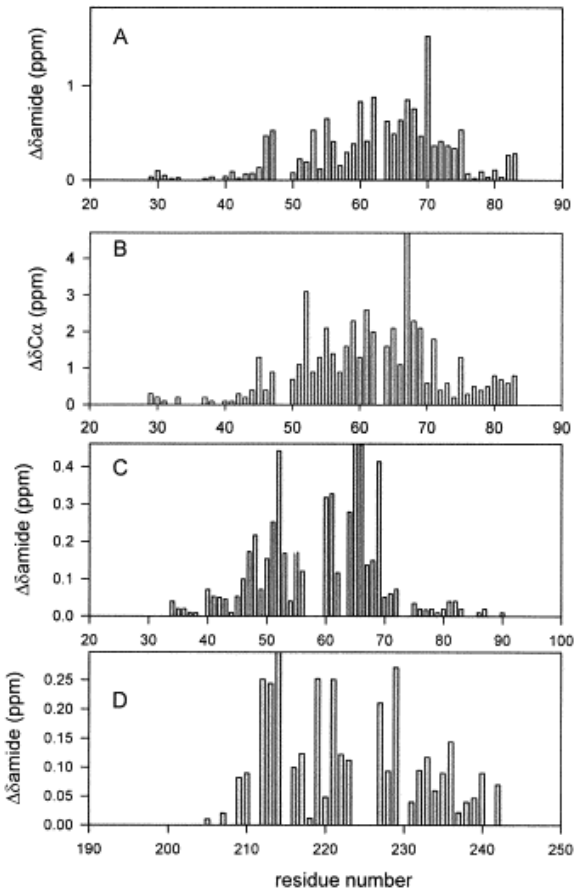

Figure 2. Chemical Shift Changes Induced by the Complexin/SNARE Complex Interaction
(A and B) Amide (A) and Cα (B) chemical shift differences between Cpx26-83 bound to the core complex and isolated complexin.
(C and D) Amide chemical shift changes induced by complexin binding on the SNARE motifs of synaptobrevin (C) and syntaxin (D) within the SNARE complex. Amide chemical shift changes were calculated as $\Delta\delta = ([\Delta\delta HN]^2 + [0.17*\Delta\delta N]^2)^{1/2}$, where ΔδHN and ΔδN are the ^1H and ^{15}N amide chemical shift changes, respectively.

To investigate which sequences of the SNARE complex are involved in binding to complexin, we prepared four samples where each SNARE motif was individually ^2H,^{15}N-labeled. We then analyzed the effects of Cpx26-83 binding on the ^1H-^{15}N TROSY-HSQC spectra of the individual SNARE motifs (Figure 3). Consistent with previous mutagenesis experiments (Pabst et al., 2000), substantial cross-peak shifts were observed for the syntaxin and synaptobrevin SNARE motifs, while only small perturbations were observed for the SNAP-25 helices. Assignment of most of the backbone resonances of the syntaxin and synaptobrevin SNARE motifs in the absence and presence of Cpx26-83 (see Figures 3A and 3B) allowed us to analyze the chemical shift changes induced in these SNARE motifs by binding to Cpx26-83 (Figures 2C and 2D, and data not shown). Only small changes in the Cα chemical shifts of synaptobrevin and syntaxin were observed upon Cpx26-83 binding (data not shown), indicating that the interaction does not induce large changes in the four-helix bundle structure of the SNARE complex. However, binding of Cpx26-83 causes considerable changes in the amide chemical shifts of the central regions of both SNARE motifs (Figures 2C and 2D). These results show that the central region of the groove between syntaxin and synaptobrevin is responsible for binding to complexin, and the approximate length of the perturbed region is consistent with the conclusion that only part of the Cpx26-83 sequence is directly involved in binding. An additional interesting observation from these experiments was that residues surrounding R56 of synaptobrevin and Q226 of syntaxin exhibit unusually broad resonances, some of which cannot be detected under the conditions of our NMR experiments. While most of the interior of the SNARE complex is hydrophobic, these two residues and two glutamines from SNAP-25 form a central polar layer whose role is highly unclear

(Sutton et al., 1998). The resonance broadening observed in this region suggests a chemical exchange process that may reflect a tendency of the SNARE complex to locally unfold around the polar layer.

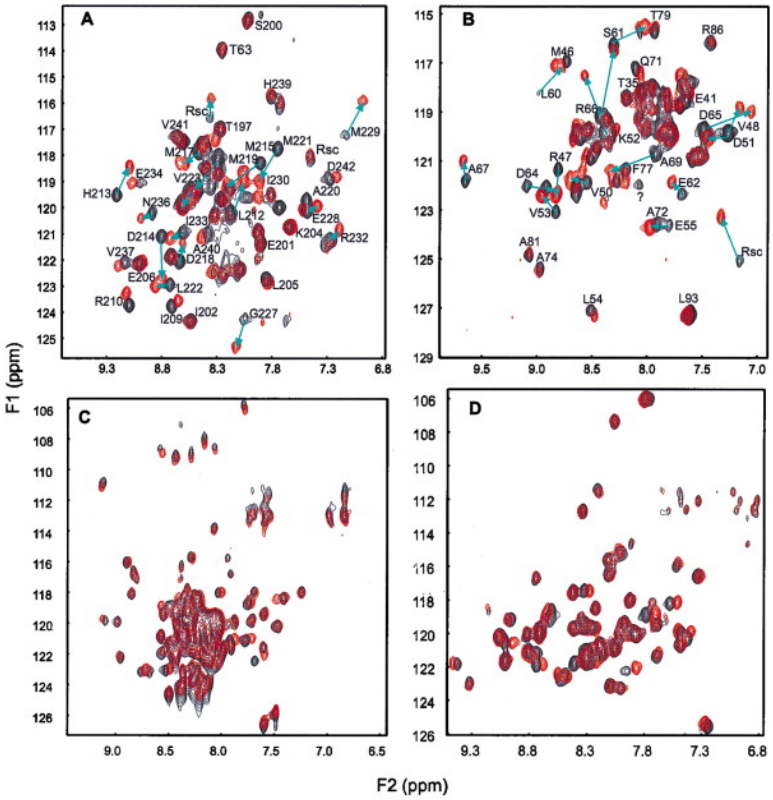

Figure 3. Changes in the ^{1}H-^{15}N TROSY-HSQC Spectra of the SNARE Complex Caused by Cpx26-83 Binding
^{1}H-^{15}N TROSY-HSQC spectra of the SNARE complex with the individual SNARE motifs of syntaxin (A), synaptobrevin (B), SNAP-25 N terminus (C), and SNAP-25 C terminus (D) ^{2}H,^{15}N-labeled in the absence (black contours) and presence (red contours) of Cpx26-83 are shown. The cross-peak assignments are indicated for the SNARE motifs of syntaxin and synaptobrevin, and the arrows illustrate the cross-peak shifts induced by Cpx26-83 binding.

Crystallization of the Complexin/SNARE Complex

To gain further insight into the nature of the interaction between complexins and the SNARE complex, we sought to crystallize the Cpx26-83/SNARE complex. Crystals that diffracted to a d_{min} of 2.5 Å were grown in 27% isopropanol at pH 7.5. This crystal form contains only one complexin/SNARE complex in the asymmetric unit. In contrast, the crystals of the isolated SNARE complex contained three complexes in the asymmetric unit (Sutton et al., 1998). This observation is consistent with the decreased tendency to aggregate caused by the C-terminal truncation of the syntaxin SNARE motif. The crystal structure of the complexin/SNARE complex was solved by molecular replacement using as a model the structure of an isolated SNARE complex and has been refined to a d_{min} of 2.5 Å. A section of the electron-density map is shown in Figure 4, and the structural statistics are described in Table 1. Only residues 32–72 from the Cpx26-83 fragment are ordered in the crystals, indicating that the 11 C-terminal residues have high mobility. This result is consistent with the sharp resonances observed for the same residues in the NMR studies of the complexin/SNARE complex described above.

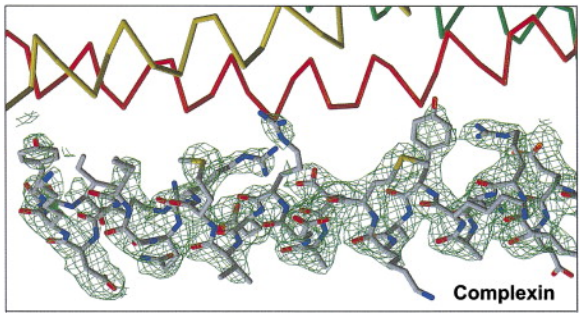

Figure 4. Experimental Electron Density of the Complexin/SNARE Complex
The complexin portion of the electron density from a composite omit map for the complexin/SNARE complex is shown; contours are drawn at 1.0 times the rms level of the map. Superimposed are the final refined coordinates for complexin and Cα traces of the SNAREs.

Table 1. Statistics of Data Collection and Refinement

Space group	**$P2_12_12_1$**
Cell dimensions	a = 40.49 Å, b = 60.42 Å, c = 159.79 Å
Number of measurements	78,881
Number of independent reflections	14,111
Data range	32.2–2.50 Å
R_{merge}:	
Overall	4.6%
Last shell (2.59–2.50 Å)	16.9%
Data completeness:	
Overall	99.6%
Last shell	99.4%
I/(σ)I:	
Overall	27.8
Last shell	6.6
Number of reflections used in refinement	13,041 (32.23–2.50 Å)
Number of non-H protein atoms	2,496
Number of water molecules, Mg^{2+}	116, 2
R_{work}	23.7%
R_{free}	30.3%
Rmsd in bond lengths	0.010 Å
Rmsd in bond angles	1.2°
Mean B value ($Å^2$):	
SNARE (all/main chain/side chain)	62.4/60.2/64.5
Complexin (all/main chain/side chain)	83.0/82.4/83.5
Complexin residues 48–70 (all/main chain/side chain)	70.3/70.8/69.9
Water molecules, Mg^{2+}:	65.5, 68.9
Cross-validated σ_A-coordinate error	0.47 Å
Missing residues	synaptobrevin: Gly27, Leu9 syntaxin: Lys191, Thr251-Lys253 snap-25 (1): Gly9, Trp82 complexin: Lys26-Ala31, Lys73-Gln83

Crystal Structure of the Complexin/SNARE Complex

The structure of the complexin/SNARE complex revealed a bundle of four parallel, highly twisted α helices formed by the SNARE motifs of synaptobrevin, syntaxin, and SNAP-25, and a fifth, slightly twisted α helix corresponding to complexin (Figure 5A). Surprisingly, the complexin helix is oriented in an antiparallel fashion with respect to the four helices formed by the SNARE motifs. A superposition of the four SNARE motifs within the complexin/SNARE complex with those of the isolated SNARE complex (Figure 5B) shows that complexin binding causes minimal structural changes. Indeed, the rms deviations between our structure and the three different complexes within the asymmetric unit of the crystals of the isolated SNARE complex range from 0.84 to 0.96 Å for 259 equivalent Cα carbons and are comparable to the corresponding rms deviations among the three structures of the isolated SNARE complex (0.53–0.92 Å). In excellent correlation with the NMR data, space-filling models of our crystal structure (Figures 5C and 5D) illustrate how the C-terminal end of the complexin helix binds to the center of the groove between synaptobrevin and syntaxin, while the N-terminal end of the helix does not directly contact the SNARE complex. This observation further confirms the conclusion that the N-terminal part of Cpx26-83 has an unusual ability to form a stable α-helical conformation even in the absence of tertiary or quaternary contacts. Note that there are no lattice contacts in the crystal that could influence the conformation of the complexin helix observed in our structure.

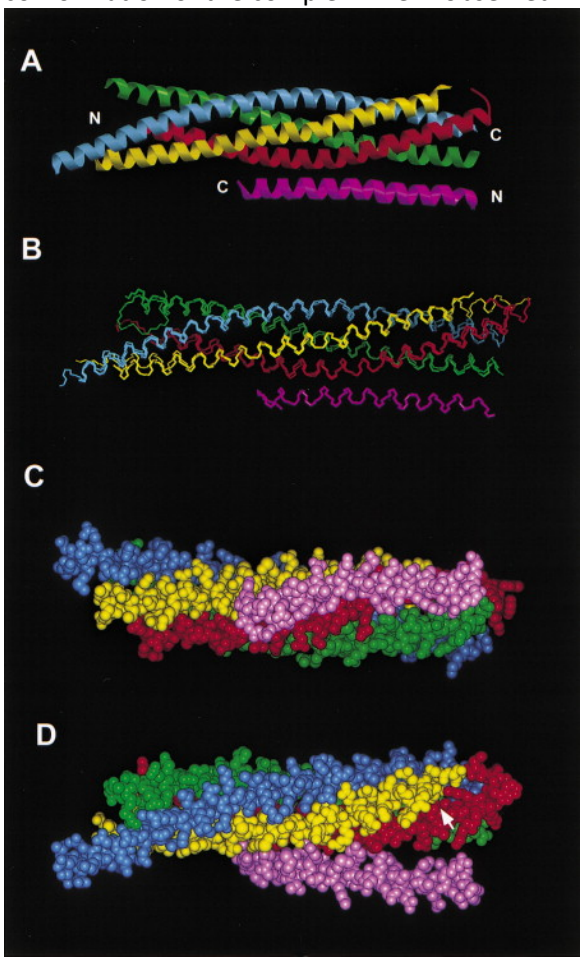

Figure 5. Structure of the Complexin/SNARE Complex

(A) Ribbon diagram with the following coloring code: yellow, syntaxin; red, synaptobrevin; blue, SNAP-25 N-terminal SNARE motif; green, SNAP-25 C-terminal SNARE motif; pink, complexin.

(B) Superposition of the structures of the isolated SNARE complex (Sutton et al., 1998) and the complexin/SNARE complex.

(C and D) Space filling models of the complexin/SNARE complex in two different views rotated approximately 90° around the horizontal axis. The white arrow in (D) indicates the position of F77 from synaptobrevin. Figure prepared with the programs InsightII (MSI) and Molscript (Kraulis, 1991).

A summary of the most important interactions that mediate binding of complexin to the SNARE complex is shown in Figure 6. Binding buries 1,666 Å^2 of solvent-accessible surface area between complexin and the SNARE complex and involves an intricate network of hydrophobic, hydrogen bonding, and ionic interactions between residues 48–70 of complexin and the sequences encompassing residues 47–68 of synaptobrevin, and residues 214–232 of syntaxin. Thus, complexin binding covers the central polar layer of the SNARE complex. Two tyrosine (Y52 and Y70) and three arginine residues (R48, R59, and R63) from complexin appear to be critical for binding to the SNARE complex. The side chain of Y52 makes extensive contacts with synaptobrevin, including a hydrogen bond with the D64 side chain, while Y70 is involved in extensive contacts with syntaxin, forming a hydrogen bond with D218. The three arginine residues of complexin form salt bridges with three aspartate residues from synaptobrevin (D57, D65, and D68) and are also involved in hydrophobic interactions. Residues M62 and I66 from complexin, V50 and L54 from synaptobrevin, and M215, L222, and M229 from syntaxin participate in additional hydrophobic interactions, while a lysine residue from complexin (K69) forms another salt bridge with an aspartate residue from syntaxin (D218).

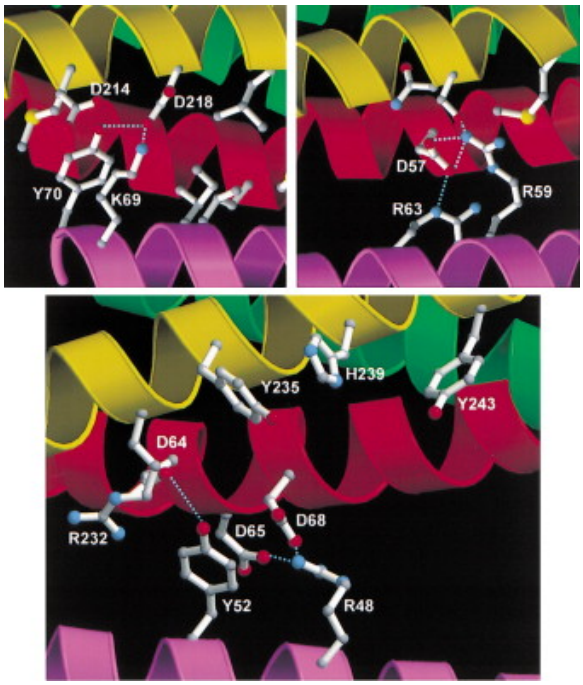

Figure 6. The Complexin/SNARE Complex Interface

Three different closeups summarizing some of the interactions between complexin and the SNARE complex are shown. The color coding for the ribbons is the same as in Figure 5. In the side chains displayed as stick-and-ball models, oxygen atoms are in red and nitrogen atoms are in blue. The bottom pannel illustrates the proximity of three stacked aromatic residues of syntaxin (Y235, H239, and Y243) to the complexin/SNARE complex interface. Figure prepared with the program Molscript (Kraulis, 1991).

The observation that the N-terminal part of the complexin helix is “hanging” isolated without making contacts with the SNARE complex (Figure 5D) is a particularly striking feature of the crystal structure. The presence of an organic solvent in our crystallization conditions could raise the concern that the organic solvent may have induced the helical conformation present in this N-terminal part or could have disrupted interactions between this region of complexin and the SNARE complex. However, the excellent agreement observed in general between the NMR data described above and the binding mode observed in the crystals validates the structure. The largest amide chemical shift changes induced in synaptobrevin and syntaxin by complexin binding (Figures

2C and 2D) correlate very well with the sequences involved in the interaction in the crystals. For the syntaxin SNARE motif, we observed substantial chemical shift changes in several residues (residues 233–243) that are beyond the complexin binding region (Figure 2D), but these changes most likely arise from the abundance of aromatic side chains in this region (Y235, H239, and Y243) (see Figure 6). Aromatic rings induce strong shifts in the resonances of neighboring nuclei and, because of the proximity of these aromatic residues to the complexin binding region, it is almost certain that complexin induces concerted alterations in their rotameric states (a comparison with the crystal structure of the isolated SNARE complex is not meaningful here because these aromatic side chains are involved in contacts between the three different complexes within the asymmetric unit). Particularly compelling evidence demonstrating the validity of the binding mode observed in the crystals is provided by the finding that most of the well dispersed cross-peaks from Cpx26-83 bound to the SNARE complex (Figure 1A) correspond to the region that makes quaternary contacts in the crystal structure and by the observation of a remarkable similarity between the N-terminal chemical shifts of Cpx26-83 bound to the SNARE complex and those of the same region in isolated complexin (see above).

Complexin Binding Stabilizes the SNARE Complex

Formation of the synaptobrevin/syntaxin interface during SNARE complex assembly is strongly opposed by the repulsive forces between the synaptic vesicle and plasma membranes. The structure of the complexin/SNARE complex suggests that complexin may act as a "tape" that seals this interface and stabilizes the assembled SNARE complex. Testing this hypothesis is difficult because the SNARE complex is extremely stable in the absence of the repulsive forces between the membranes. Thus, the SNARE complex is SDS resistant (Hayashi et al., 1994) and can only be denatured at high temperatures (more than 90°C; Fasshauer et al., 1997) or in saturating concentrations of urea or guanidinium chloride. These harsh conditions disrupt the complexin/SNARE complex interaction before they have any effect on the SNARE complex and, consequently, complexin does not affect the denaturation curves observed for the SNARE complex (our unpublished data). In addition, global unfolding of the SNARE complex is infinitely slow for practical purposes at room temperature in the absence of denaturants (Fasshauer et al., 1999). However, deuterium exchange experiments Kim et al. 1993, Englander and Hiller 2001 provide a sensitive tool to probe partial unfolding associated with thermal motions of the individual helices within the assembled SNARE complex. These experiments can thus yield information on local energetic contributions to the stability of the complex and can be performed under nondenaturing conditions. Of particular interest are the local interactions involving synaptobrevin since establishing these interactions with syntaxin/SNAP-25 complexes, which are believed to be preassembled at the plasma membrane Nicholson et al. 1998, Fiebig et al. 1999, Misura et al. 2001, Xiao et al. 2001, is likely to constitute the final step in SNARE complex formation. These arguments led us to test our hypothesis by investigating the effects that complexin binding has on the kinetics of deuterium exchange of individual synaptobrevin amide protons within the SNARE complex.

To monitor deuterium exchange, we used ^{1}H-^{15}N TROSY-HSQC spectra of samples of the SNARE complex where only the synaptobrevin SNARE motif was ^{2}H,^{15}N-labeled. Hence, these spectra contain cross-peaks for only the amide groups of the synaptobrevin SNARE motif. Upon placing the complex in D_2O, deuterium exchange with the solvent results in progressive deuteration of the amide groups and, thus, concomitant disappearance of their corresponding cross-peaks in the ^{1}H-^{15}N TROSY-HSQC spectrum. The ratios between the observed deuterium exchange rates and those expected for the same sequence in a random coil (Bai et al., 1993) are known as protection factors and reflect the levels of protection of the amide groups against exchange with the solvent due to formation of a defined three-dimensional structure. Due to the unusual stability of the SNARE complex, high protection factors were expected for at least some of the amide protons of synaptobrevin. Hence, the deuterium exchange experiments were performed under conditions that favor fast amide exchange ([pH 7.5], 30°C; see Bai et al., 1993) to better distinguish the stability in different parts of the synaptobrevin sequence within the SNARE complex. Figures 7A and 7B show the ^{1}H-^{15}N TROSY-HSQC spectra obtained after 7 days of deuterium exchange in the absence or presence of Cpx26-83, and a summary of the amide protons that were still observable is shown in Figure 7C. The protection factors estimated for these amide protons are

approximately 10^7 or larger. Such protection factors indicate a remarkable resistance to local unfolding, considering the fact that there is a substantial amount of solvent-accessible surface area along the whole synaptobrevin helix even after complexin binding.

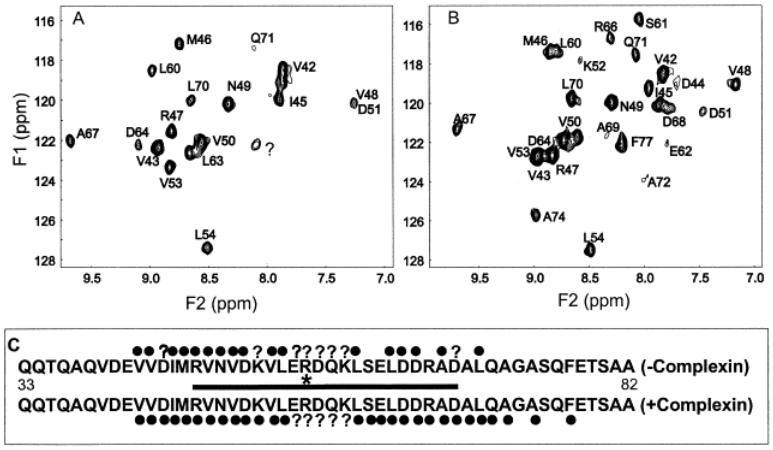

Figure 7. Complexin Stabilizes the Synaptobrevin/Syntaxin Interface
(A and B) $^{1}H,^{15}N$-TROSY-HSQC spectra of the SNARE complex with only the synaptobrevin motif $^{2}H,^{15}N$-labeled in the absence (A) or presence (B) of Cpx26-83 after 7 days at 30°C in D_2O (pD 7.5).
(C) Summary of the protection against deuterium exchange of the amide protons from synaptobrevin within the SNARE complex in the absence or presence of Cpx26-83. Bullets indicate residues whose amide protons remain observable after 7 days of deuterium exchange and, thus, are highly protected. Question marks indicate residues that were not assigned or that cannot be monitored due to cross-peak overlap. The star indicates Arg56, which is part of the polar layer. The bar indicates the region of complexin involved in binding to the SNARE complex.

The deuterium exchange experiments performed with the isolated SNARE complex showed that, as expected, the least protected regions of the synaptobrevin SNARE motif correspond to both the N termini and C termini since local unfolding should more easily originate at the ends of the complex. These experiments also showed that a region N-terminal to the polar layer (residues 42–54 of synaptobrevin) is highly protected against exchange (Figures 7A and 7C), indicating that this region contains very stable contacts between synaptobrevin and the rest of the SNARE complex. On the other hand, the region immediately C-terminal to the polar layer contains a few highly protected residues, but the protection pattern is fragmented, suggesting the existence of local unfolding events that are uncoupled from those originating at the termini. Such events could arise from the polar layer, since very broad resonances are observed around this region, and might be important for SNARE complex disassembly.

Upon addition of complexin, strong protection on both sides of the polar layer was observed (Figures 7B and 7C). This result is due at least in part to the existence of quaternary contacts between complexin and residues 47–68 of synaptobrevin, which should hinder local unfolding in this region. However, the observation that additional C-terminal residues beyond the binding region also become protected upon complexin binding shows that the stabilization caused by complexin propagates toward the C terminus of the SNARE complex. Note that the strong protection observed for F77 is amazing since this residue is very close to the C-terminal end of the SNARE complex (see white arrow in Figure 5D) where the natural tendency of the complex to fray at the termini is likely increased by the truncation of the syntaxin SNARE motif. This observation indicates that extremely tight contacts between synaptobrevin and syntaxin/SNAP-25 exist at the C terminus of the SNARE complex. Such contacts are close to the site of membrane merger and may be critical to pull the membranes together. The lesser protection of this C-terminal region against exchange in the absence of complexin most likely arises from the local unfolding events originating at sequences closer to the polar layer, and such events are prevented by

complexin binding. Thus, our results reveal unsuspected dynamic aspects of the SNARE complex and demonstrate that complexin binding indeed stabilizes the interface between synaptobrevin and syntaxin.

Discussion

Extensive studies of the neuronal SNARE proteins have led to a working model for their function in neurotransmitter release whereby formation of the highly stable SNARE complex drives the synaptic vesicle and plasma membranes together. However, the steps that lead to neurotransmitter release and the functions of additional proteins that are critical for this process are still poorly understood. Among these proteins, complexin is particularly intriguing because of its tight interaction with the assembled SNARE complex (McMahon et al., 1995). Previous studies had highlighted the importance of complexin for neurotransmitter release and for survival itself (Reim et al., 2001) and had yielded important clues on how this protein interacts with the SNARE complex (Pabst et al., 2000). However, it was difficult to reconcile the observation that the complexin/SNARE complex interaction is Ca^{2+} independent with the selective decrease in Ca^{2+}-evoked neurotransmitter release observed in complexin knockout mice. Taking advantage of the different strengths of X-ray crystallography and NMR spectroscopy, the studies of the complexin/SNARE complex described here yield a structure at atomic resolution of a SNARE-interacting protein bound to the core complex and bring insights into the function of this protein. Our results provide a detailed picture of how complexin binds in an antiparallel α-helical conformation to the groove between synaptobrevin and syntaxin and stabilizes the interface between these two SNAREs that bears the repulsive forces between the apposed membranes.

Our NMR and X-ray data show that, upon binding of complexin to the SNARE complex, the backbone structure of the four-helix bundle formed by the SNAREs is not altered, and most of the Cpx26-83 sequence forms a straight α helix that ends abruptly at a helix-breaking residue (Gly71). Surprisingly, however, the interaction involves only residues 48–70 of complexin. The N-terminal part of Cpx26-83 does not make direct contact with the four-helix bundle. Our previous NMR studies had shown that, in isolated complexin, the N-terminal part of residues 26–83 forms a remarkably stable α helix, while the C-terminal part exhibits a much lower population of helical conformation (Pabst et al., 2000). Thus, this N-terminal sequence seems to be designed to indirectly increase the affinity of the interaction by helping to nucleate a helical conformation toward the C terminus, where residues with a lower helical propensity are optimized for binding to the synaptobrevin/syntaxin interface. The resulting complex cannot be considered a five-helix bundle since there is no symmetrical relation between the five α helices, but, rather, reflects a recognition event between a partially induced α helix and a groove within a four-helix bundle. Such recognition involves multiple ionic, hydrogen bonding, and hydrophobic interactions along the center of the synaptobrevin/syntaxin interface, suggesting that complexin seals this interface acting like a “tape”.

The structure of the complexin/SNARE complex provides a framework to understand the function of complexin in combination with the available biochemical and genetic data. One model proposed recently suggested that complexin induces SNARE complex oligomerization by reshuffling the two SNARE motifs of SNAP-25 into separate SNARE complexes and that cysteine residues in the loop connecting the two SNARE motifs were involved in the oligomerization (Tokumaru et al., 2001). However, this model seems highly unlikely since: (1) the model assumed that complexin would cause a structural change in the SNARE complex and no such change was observed from our NMR and X-ray data, (2) the presence or absence of the SNAP-25 loop does not affect the interaction between complexin and the SNARE complex (Pabst et al., 2000), (3) neither oligomerization mediated by the SNAP-25 SNARE motifs nor the cysteine residues in the connecting loop are required for exocytosis in PC12 cells Chen et al. 1999, Scales et al. 2000, and (4) SNAP-25 has a high tendency to oligomerize via cysteine oxidation and no precautions to avoid such oxidation were described in the study of Tokumaru et al. (2001). This study also suggested that complexin could play a role in assisting SNARE complex assembly, but the results leading to this proposal were surprising since little SNARE complex assembly was observed in the absence of complexin (Tokumaru et al., 2001), while the SNARE complex is known to assemble efficiently without the need for complexin (e.g., Fasshauer et al., 1997).

The mode of interaction between complexin and the SNARE complex observed in our structure led us to formulate an alternative model whereby complexin functions by binding to the assembled SNARE complex and stabilizing the synaptobrevin/syntaxin interface that bears the repulsion between the synaptic vesicle and plasma membranes. Deuterium exchange experiments monitored by NMR spectroscopy provided a powerful tool to show that complexin binding indeed stabilizes the synaptobrevin/syntaxin interface and that such stabilization extends beyond the interacting region toward the C terminus where the membrane anchors are located. Based on these results, together with the phenotype observed in complexin knockout mice (Reim et al., 2001), we propose that stabilization of the assembled SNARE complex by complexin binding represents a critical step to ensure efficient, fast neurotransmitter release upon Ca^{2+} influx (Figure 8). Why would fast neurotransmitter release require a protein such as complexin as opposed to other types of intracellular membrane fusion that do not require complexin?

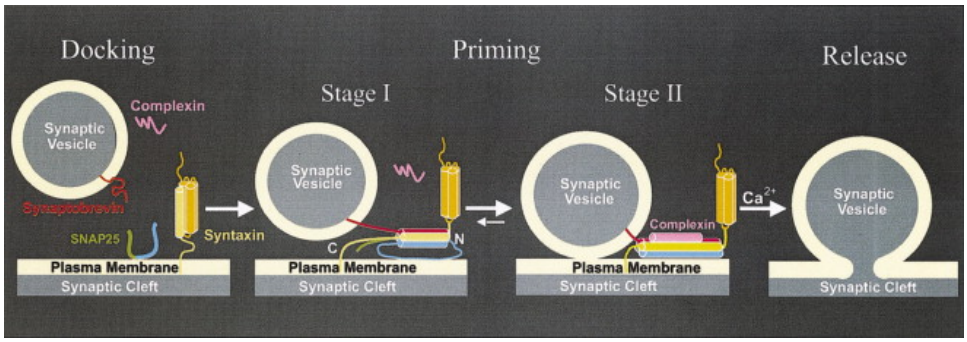

Figure 8. Model for the Function of Complexin in Neurotransmitter Release
The primary proposals of this model are: (1) that synaptic vesicle priming occurs in two stages and (2) that complexin stabilizes the second, fully primed state with a fully assembled SNARE complex as a critical step to leave the exocytotic machinery ready for fast neurotransmitter release upon Ca^{2+} influx (see Discussion for details). All proteins are colored coded as in Figure 5, except that the three-helix N-terminal domain of syntaxin (Fernandez et al., 1998), which is not present in our structure, is colored in orange. In the docking step, syntaxin is represented in a "closed conformation" where the SNARE motif is bound to the three-helix bundle (see Nicholson et al. 1998, Fiebig et al. 1999, Dulubova et al. 1999).

Models where the SNARE complex assembles in different steps starting at the N terminus and "zippering up" toward the C terminus have been proposed previously in different contexts (e.g., Geppert and Südhof 1998, Fiebig et al. 1999, Xu et al. 1999). Such models are inspired by the natural assumption that assembly of the C-terminal part of the SNARE complex should be the last step in attracting the membranes together. Our deuterium exchange data indicate that the N-terminal half of the SNARE complex is indeed highly stable, and, hence, it is easy to envision that this N-terminal half can initially assemble while the C-terminal half remains unengaged because of repulsion between the membranes. Full SNARE complex assembly may lead to a metastable state that perhaps involves membrane hemifusion. Constitutive membrane fusion may occur in a probabilistic fashion whereby this metastable state forms transiently and most often reverts back to the half-assembled state but occasionally proceeds toward full fusion. This probabilistic process could result in a high-fusion efficiency at long time scales but a low probability of fusion over short time scales such as those characteristic of fast neurotransmitter release (<1 ms). Our model proposes that the metastable state with a fully preassembled SNARE complex is essential for neurotransmitter release to meet such stringent time requirements upon Ca^{2+} influx and that complexin is critical to stabilize the assembled SNARE complex, helping to keep a high population of this metastable state.

The model shown in Figure 8 is based on these arguments and represents an attempt to integrate the available data on SNAREs and complexin with the electrophysiology of neurotransmitter release, although the model needs to be considered an oversimplification since other proteins such as munc18-1 and synaptotagmin 1 are

critical for this process. It is generally believed that synaptic vesicles first dock to the plasma membrane in a SNARE-independent manner and then undergo a priming reaction that leaves them ready for release upon Ca^{2+} influx (Südhof, 1995). The readily-releasable pool of vesicles is commonly associated with the vesicles that have been primed and can be released by hypertonic sucrose treatment. However, it is conceivable that priming occurs in more than one step. We envision that the first step of priming involves assembly of the N-terminal half of the SNARE complex after releasing the inhibition caused by intramolecular binding of the N-terminal domain of syntaxin to its SNARE motif (Figure 8) (see Nicholson et al. 1998, Fiebig et al. 1999, Dulubova et al. 1999). In our model, the second priming step involves formation of the metastable state with a fully assembled SNARE complex; this state is stabilized by complexin and is essential for efficient, fast, Ca^{2+}-dependent neurotransmitter release. This model offers a plausible explanation for the observation that hypertonic sucrose treatment is not affected in the complexin knockout (Reim et al., 2001) since both primed states could be released by this treatment, and for the enigmatic observation that complexin binding to the SNARE complex is Ca^{2+} independent, while deletion of complexin causes a selective decrease in fast Ca^{2+}-dependent neurotransmitter release.

Clearly, alternative models of complexin function can be proposed. For instance, full SNARE complex assembly might occur only after Ca^{2+} influx, and stabilization of the fully assembled SNARE complex by complexin binding could extend its half-life, thereby increasing the probability of membrane fusion. Whether the stabilization effect occurs before or after Ca^{2+} influx, it is tempting to speculate from our model that regulation of the levels of expression of complexin could provide a mechanism to regulate the efficiency of Ca^{2+}-evoked neurotransmitter release during processes of presynaptic plasticity that may underly information processing in the brain. The structure of the complexin/SNARE complex described here now provides a framework to test these models and to rationalize further studies of the function of complexin and the SNAREs.

Experimental Procedures

Protein Expression and Purification

DNA encoding GST fusion proteins of the complexin 1 fragment (residues 26–83) and the SNARE motifs of synaptobrevin 2 (residues 29–93), syntaxin 1A (residues 191–253), and SNAP-25 (residues 11–82 and 141–203, both including an additional Trp residue at the C terminus to facilitate detection) were made using custom-designed primers and standard PCR cloning techniques and subcloned into the pGEX-KT expression vector (Hakes and Dixon, 1992). The fusion proteins were expressed in *E. coli* BL21(DE3), isolated by affinity chromatography on glutathione-agarose (Sigma), cleaved with thrombin, and purified by gel filtration, except Cpx26-83, which was purified by anion exchange chromatography on Source-S (Pharmacia). Uniform ^{15}N- and ^{13}C-labeling was achieved by growing the bacteria in $^{15}NH_4Cl$ and $^{13}C_6$-glucose as the sole nitrogen and carbon sources, respectively. Perdeuteration was achieved by growing bacteria using D_2O as the solvent.

SNARE Complex and Complexin/SNARE Complex Preparation

The high stability of the SNARE complex allowed facile preparation by simple mixing of stoichiometric amounts of the four purified SNARE motifs, followed by an overnight incubation and extensive concentration/dilution with a Millipore concentrator (10 kDa cutoff) to eliminate small amounts of uncomplexed fragments. This procedure yielded pure SNARE complex as judged by SDS-PAGE. Note that the complex is SDS resistant, and the absence of isolated SNARE bands in the gel provide a reliable method to assess the purity of the complex. The complexin/SNARE complex was prepared by addition of 1.2 equivalents of Cpx26-83 to preassembled SNARE complex followed by extensive concentration/dilution after incubating for 2 hr. The purity of the complex was checked by nondenaturing PAGE. The observation of only one set of cross-peaks in the ^{1}H-^{15}N TROSY-HSQC spectra of the different samples prepared Figure 1, Figure 3 provided further evidence for the purity of both complexes.

NMR Spectroscopy

All NMR samples were prepared in 20 mM Tris (pH 7.4) containing 250 mM NaCl. Samples for ^{1}H-^{15}N TROSY-HSQC spectra of SNARE complexes and complexin/SNARE complexes with individual helices ^{2}H,^{15}N-labeled contained 100 µM complex. The concentrations of samples for resonance assignments were between 170 and 300 µM. Two SNARE complexes where either the syntaxin or the synaptobrevin SNARE motif was ^{2}H,^{15}N,^{13}C-labeled were used to obtain the assignments for the corresponding SNARE motifs before and after addition of Cpx26-83. An additional complexin/SNARE complex where the Cpx26-83 fragment was ^{2}H,^{15}N,^{13}C-labeled was used to assign the resonances of Cpx26-83 bound to the SNARE complex. All NMR experiments were performed on Varian INOVA500 or INOVA600 spectrometers at 32°C, except ^{1}H-^{15}N TROSY-HSQC spectra for deuterium exchange experiments, which were acquired at 30°C. The resonance assignments were obtained from the sequential NH/NH NOEs observed in 3D ^{1}H-^{15}N NOESY-HSQC spectra (Zhang et al., 1994) in combination with analysis of TROSY-HNCA and TROSY-HN(CO)CA acquired with ^{2}H-decoupling (Yang and Kay, 1999). All NMR data were processed with the program NMRPipe (Delaglio et al., 1995) and analyzed with the program NMRView (Johnson and Blevins, 1994).

Complexin/SNARE Complex Crystallization

Assembled complexin/SNARE complex dissolved in 20 mM Tris (pH 7.5), and 130 mM NaCl was concentrated to 10 mg/ml and stored in small aliquots at −80°C. Tiny trigonal bipyramidal crystals grew spontaneously at 4°C in hanging drop vapor diffusion experiments upon mixing equal volumes of complexin/SNARE complex stock solution and reservoir solution consisting of 35% (v/v) isopropanol, 200 mM $MgCl_2$, 100 mM HEPES (pH 7.5). Diffraction quality crystals were obtained after streak seeding of equilibrated drops containing 27% (v/v) isopropanol, 200 mM $MgCl_2$, 100 mM HEPES (pH 7.5) in the reservoir. Crystals were transferred to fresh reservoir solution at 4°C containing 20% glycerol as cryoprotectant and flash cooled in liquid propane, then stored in liquid nitrogen until used for data collection.

Data Collection

Diffraction data were initially collected to a d_{min} of 3.4 Å from a 20 µm single crystal at 110K using an R axis IV imaging plate system (MSC, Houston, TX) mounted on a Rigaku RU-200 rotating anode (CuKα) (Rigaku, Japan) operated at 100 mA and 50 kV. These data were used for the initial structure solution. Subsequently, a complete data set was collected to a d_{min} of 2.5 Å from a 200 µm single crystal at 100K at the Structural Biology Center 19–ID beamline of the Advanced Photon Source with the use of the SBC 2 CCD detector (Naday et al., 1998). This crystal displayed anisotropic diffraction. The complexin/SNARE complex crystallized with the symmetry of space group $P2_12_12_1$ (unit cell constants a = 40.49 Å, b = 60.42 Å, c = 159.79 Å) with one molecule per asymmetric unit. All data were processed and scaled in the HKL2000 program suite (Otwinowski and Minor, 1997). Intensities were converted to structure factor amplitudes and placed on an approximate absolute scale by the program TRUNCATE from the CCP4 package French and Wilson 1978, CCP 4 1994. The Wilson B value calculated for the observed data between a d_{min} of 4.0 and 2.5 Å was 53 $Å^2$. Data collection and processing statistics are summarized in Table 1.

Crystallographic Structure Solution and Refinement

The complexin/SNARE complex structure was solved via molecular replacement using the program AMORE (Navaza, 1994). Initial model coordinates were obtained by modifying the coordinates of the SNARE complex (PDB code 1sfc) (Sutton et al., 1998) by removing the coordinates of residues at both the N termini and C termini of each protein that were not included in the construct. The rotation and translation function search was conducted between a d_{min} of 8.0 and 4.0 Å, and a single solution was obtained with a final correlation coefficient of 0.39. Rigid-body refinement of the coordinates from this solution versus data between a d_{min} of 20.0 and 3.4 Å was conducted in the program package CNS 1.0 (Brünger et al., 1998) with a random 5% subset of all data set aside for an R_{free} calculation. Examination of the resulting electron density map in the program O (Jones et al., 1991) revealed extra density at the C-terminal end of the SNARE complex four-helix bundle. This density was

clearly α-helical, but the side chain density was very weak; thus, it was not possible to determine the correct orientation of the complexin helix. Subsequent rigid-body refinement of the molecular replacement solution was conducted versus the synchrotron data between a d_{min} of 20.0 and 2.5 Å. The density for the complexin helix in the resulting electron density map was easily interpretable in terms of orientation and sequence (Figure 4).

All refinement calculations were performed in the program CNS 1.10. One cycle of simulated annealing refinement of the complexin/SNARE model was followed by a cycle of standard positional and group isotropic atomic displacement parameter refinement. Subsequent cycles of standard positional and individual isotropic atomic displacement parameter refinement coupled with cycles of model rebuilding and addition of solvent molecules were carried out against all data from 32.2 to 2.5 Å. The current model has free and working R values of 30.3% and 23.7%, respectively, against the experimental data. There are no outliers in the Ramachandran plot. Complete refinement statistics for the structure are listed in Table 1. The mean B values for the SNARE complex are in accord with the Wilson B value for the observed data, while the higher mean B values for complexin may reflect the lower degree of order due to the smaller interaction surface with the SNARE complex. Note that significantly smaller mean B values are observed for the residues of complexin that contact the SNARE complex (residues 48–70).

Acknowledgements

We thank Tara Murphy for excellent technical assistance; Irina Dulubova for help in the preparation of expression vectors; Reinhard Jahn, Dirk Fasshauer, and Stefan Pabst for fruitful discussions and assistance in the procedures for SNARE complex assembly; Lewis Kay for providing pulse sequences; Ranjith Muhandiram for assistance in setting up NMR experiments; and Andrzej Joachimiak and the staff of the Structural Biology Center beamline (19 ID) at the Advanced Photon Source for assistance in X–ray data collection. Use of the Argonne National Laboratory Structural Biology Center beamlines at the Advanced Photon Source was supported by the U.S. Department of Energy, Office of Biological and Environmental Research, under Contract No. W-31-109-ENG-38. This work was supported by an Established Investigator Grant from the American Heart Association and by NIH grant NS37200 (to J.R.).

Accession Numbers

Coordinates have been deposited with the Protein Data Bank under the accession code 1KIL.

References

Bai et al. 1993 Y. Bai, J.S. Milne, L. Mayne, S.W. Englander **Primary structure effects on peptide group hydrogen exchange** Proteins, 17 (1993), pp. 75-86

Brünger et al. 1998 A.T. Brünger, P.D. Adams, G.M. Clore, W.L. DeLano, P. Gros, R.W. Grosse-Kunstleve, J.S. Jiang, J. Kuszewski, M. Nilges, N.S. Pannu, *et al.* **Crystallography & NMR system: a new software suite for macromolecular structure determination** Acta Crystallogr. D Biol. Crystallogr., 54 (1998), pp. 905-921

Chen et al. 1999 Y.A. Chen, S.J. Scales, S.M. Patel, Y.-C. Doung, R.H. Scheller **SNARE complex formation is triggered by Ca^{2+} and drives membrane fusion** Cell, 97 (1999), pp. 165-174

CCP 4 1994 CCP4 **Collaborative Computational Project, Number 4) The CCP4 suite programs for protein crystallography** Acta Crystallogr. D, 50 (1994), pp. 70-763

Delaglio et al. 1995 F. Delaglio, S. Grzesiek, G.W. Vuister, G. Zhu, J. Pfeifer, A. Bax **NMRpipe: a multidimensional spectral processing system based on UNIX pipes** J. Biomol. NMR, 6 (1995), pp. 277-293

Dulubova et al. 1999 I. Dulubova, S. Sugita, S. Hill, M. Hosaka, I. Fernandez, T.C. Südhof, J. Rizo **A conformational switch in syntaxin during exocytosis: role of munc18** EMBO J., 18 (1999), pp. 4372-4382

Eastwood and Harrison 2000 S.L. Eastwood, P.J. Harrison **Hippocampal synaptic pathology in schizophrenia, bipolar disorder and major depression: a study of complexin mRNAs** Mol. Psychiatry, 5 (2000), pp. 425-432

Englander and Hiller 2001 S.W. Englander, R. Hiller **Dynamics and thermodynamics of hyperthermophilic proteins by hydrogen exchange** Methods Enzymol., 334 (2001), pp. 342-350

Fasshauer et al. 1997 D. Fasshauer, H. Otto, W.K. Eliason, R. Jahn, A.T. Brunger **Structural changes are associated with soluble N-ethylmaleimide-sensitive fusion protein attachment protein receptor complex formation** J. Biol. Chem., 272 (1997), pp. 28036-28041

Fasshauer et al. 1999 Fasshauer, D., Langen, R., Margittai, M., and Jahn, R. (1999). Structural studies on SNARE complex association and dissociation. In International Meeting on Transport of Proteins and Membranes in Eukariotic Cells, Gottingen, Germany.

Fernandez et al. 1998 I. Fernandez, J. Ubach, I. Dulubova, X. Zhang, T.C. Südhof, J. Rizo **Three-dimensional structure of an evolutionary conserved N-terminal domain of syntaxin 1A** Cell, 94 (1998), pp. 841-849

Fiebig et al. 1999 K.M. Fiebig, L.M. Rice, E. Pollock, A.T. Brunger **Folding intermediates of SNARE complex assembly** Nat. Struct. Biol., 6 (1999), pp. 117-123

French and Wilson 1978 S. French, K. Wilson **On the treatment of negative intensity observations** Acta Crystallogr., A34 (1978), pp. 517-525

Geppert and Südhof 1998 M. Geppert, T.C. Südhof **RAB3 and synaptotagmin: the yin and yang of synaptic membrane fusion** Annu. Rev. Neurosci., 21 (1998), pp. 75-95

Hakes and Dixon 1992 D.J. Hakes, J.E. Dixon **New vectors for high lever expression of recombinant protein in bacteria** Anal. Biochem., 202 (1992), pp. 293-298

Hanson et al. 1997 P.I. Hanson, R. Roth, H. Morisaki, R. Jahn, J.E. Heuser **Structure and conformational changes in NSF and its membrane receptor complexes visualized by quick-freeze/deep-etch electron microscopy** Cell, 90 (1997), pp. 523-535

Hayashi et al. 1994 T. Hayashi, H. McMahon, S. Yamasaki, T. Binz, Y. Hata, T.C. Südhof, H. Niemann **Synaptic vesicle membrane fusion complex: action of clostridial neurotoxins on assembly** EMBO J., 13 (1994), pp. 5051-5061

Ishizuka et al. 1995 T. Ishizuka, H. Saisu, S. Odani, T. Abe **Synaphin: a protein associated with the docking/fusion complex in presynaptic terminals** Biochem. Biophys. Res. Commun., 213 (1995), pp. 1107-1114

Jahn and Südhof 1999 R. Jahn, T.C. Südhof **Membrane fusion and exocytosis** Annu. Rev. Biochem., 68 (1999), pp. 863-911

Johnson and Blevins 1994 B.A. Johnson, R.A. Blevins **NMRView: a computer program for visualization and analysis of NMR data** J. Biomol. NMR, 4 (1994), pp. 603-614

Jones et al. 1991 T.A. Jones, J.Y. Zou, S.W. Cowan, M. Kjeldgaard **Improved methods for building protein models in electron density maps and the location of errors in these models** Acta Crystallogr., A47 (1991), pp. 110-119

Kraulis 1991 P.J. Kraulis **Molscript: a program to produce both detailed and schematic plots of protein structures** J. Appl. Crystallogr., 24 (1991), pp. 946-950

Kim et al. 1993 K.S. Kim, J.A. Fuchs, C.K. Woodward **Hydrogen exchange identifies native-state motional domains important in protein folding** Biochemistry, 32 (1993), pp. 9600-9608

Lin and Scheller 2000 R.C. Lin, R.H. Scheller **Mechanisms of synaptic vesicle exocytosis** Annu. Rev. Cell Dev. Biol., 16 (2000), pp. 19-49

Margittai et al. 2001 M. Margittai, D. Fasshauer, S. Pabst, R. Jahn, R. Langen **Homo- and heterooligomeric SNARE complexes studied by site-directed spin labeling** J. Biol. Chem., 276 (2001), pp. 13169-13177

McMahon et al. 1995 H.T. McMahon, M. Missler, C. Li, T.C. Südhof **Complexins: cytosolic proteins that regulate SNAP receptor function** Cell, 83 (1995), pp. 111-119

Misura et al. 2001 K. Misura, L.C. Gonzalez Jr., A.P. May, R.H. Scheller, W.I. Weis **Crystal structure and biophysical properties of a complex between the N-terminal SNARE region of SNAP25 and syntaxin 1A** J. Biol. Chem., 276 (2001), pp. 41301-41309

Morton and Edwardson 2001 A.J. Morton, J.M. Edwardson **Progressive depletion of complexin II in a transgenic mouse model of Huntington's disease** J. Neurochem., 76 (2001), pp. 166-172

Naday et al. 1998 I. Naday, S. Ross, E.M. Westbrook, G. Zentai **Charge-coupled device/fiber optic taper array X-ray detector for protein crystallography** Optical Engineering, 37 (1998), pp. 1235-1244

Navaza 1994 J. Navaza **AmoRe: an automated package for molecular replacement** Acta Crystallogr., A50 (1994), pp. 157-163

Nicholson et al. 1998 K.L. Nicholson, M. Munson, R.B. Miller, T.J. Filip, R. Fairman, F.M. Hughson **Regulation of SNARE complex assembly by an N-terminal domain of the t-SNARE Sso1p** Nat. Struct. Biol., 5 (1998), pp. 793-802

Otwinowski and Minor 1997 Z. Otwinowski, W. Minor **Processing of x-ray diffraction data collected in oscillation mode** Methods Enzymol., 276 (1997), pp. 307-326

Pabst et al. 2000 S. Pabst, J. Hazzard, W. Antonin, T.C. Südhof, R. Jahn, J. Rizo, D. Fasshauer **Selective interaction of complexin with the neuronal SNARE complex** J. Biol. Chem., 275 (2000), pp. 19808-19818

Pelham 1999 H.R. Pelham **SNAREs and the secretory pathway-lessons from yeast** Exp. Cell Res., 247 (1999), pp. 1-8

Pervushin et al. 1997 K. Pervushin, R. Riek, G. Wider, K. Wüthrich **Attenuated T2 relaxation by mutual cancellation of dipole-dipole coupling and chemical shift anisotropy indicates an avenue to NMR structures of very large macromolecules in solution** Proc. Natl. Acad. Sci. USA, 94 (1997), pp. 12366-12371

Reim et al. 2001 K. Reim, M. Mansour, F. Varoqueaux, H.T. McMahon, T.C. Südhof, N. Brose, C. Rosenmund **Complexins regulate a late step in Ca^{2+}-dependent neurotransmitter release** Cell, 104 (2001), pp. 71-81

Scales et al. 2000 S.J. Scales, Y.A. Chen, B.Y. Yoo, S.M. Patel, Y.-C. Doung, R. Scheller **SNAREs contribute to the specificity of membrane fusion** Neuron, 26 (2000), pp. 457-464

Schoch et al. 2001 S. Schoch, F. Deak, A. Konigstorfer, M. Mozhayeva, Y. Sara, T.C. Südhof, E. Kavalali **SNARE function analyzed in synaptobrevin/VAMP knockout mice** Science, 294 (2001), pp. 1117-1122

Söllner et al. 1993 T. Söllner, M.K. Bennet, S.W. Whiteheart, R.H. Scheller, J.E. Rothman **A protein assembly-disassembly pathway in vitro that may correspond to sequential steps of synaptic vesicle docking, activation, and fusion** Cell, 75 (1993), pp. 409-418

Südhof 1995 T.C. Südhof **The synaptic vesicle cycle: a cascade of protein-protein interactions** Nature, 375 (1995), pp. 645-653

Sutton et al. 1998 R.B. Sutton, D. Fasshauer, R. Jahn, A.T. Brunger **Crystal structure of a SNARE complex involved in synaptic exocytosis at 2.4 Å resolution** Nature, 395 (1998), pp. 347-353

Takahashi et al. 1995 S. Takahashi, H. Yamamoto, Z. Matsuda, M. Ogawa, K. Yagyu, T. Taniguchi, T. Miyata, H. Kaba, T. Higuchi, F. Okutani, S. Fujimoto **Identification of two highly homologous presynaptic proteins distinctly localized at the dendritic and somatic synapses** FEBS Lett., 368 (1995), pp. 455-460

Tokumaru et al. 2001 H. Tokumaru, K. Umayahara, L.L. Pellegrini, T. Ishizuka, H. Saisu, H. Betz, G.J. Augustine, T. Abe **SNARE complex oligomerization by synaphin/complexin is essential for synaptic vesicle exocytosis** Cell, 104 (2001), pp. 421-432

Ungermann et al. 1998 C. Ungermann, K. Sato, W. Wickner **Defining the functions of trans-SNARE pairs** Nature, 396 (1998), pp. 543-548

Weber et al. 1998 T. Weber, B.V. Zemelman, J.A. McNew, B. Westermann, M. Gmachl, F. Parlati, T.H. Söllner, J.E. Rothman **SNAREpins: minimal fusion machinery for membrane fusion** Cell, 92 (1998), pp. 759-772

Xiao et al. 2001 W. Xiao, M.A. Poirier, M.K. Bennett, Y.K. Shin **The neuronal t-SNARE complex is a parallel four-helix bundle** Nat. Struct. Biol., 8 (2001), pp. 308-311

Xu et al. 1999 T. Xu, B. Rammner, M. Margittai, A.R. Artalejo, E. Neher, R. Jahn **Inhibition of SNARE complex assembly differentially affects kinetic components of exocytosis** Cell, 99 (1999), pp. 713-722

Yang and Kay 1999 D. Yang, L.E. Kay **TROSY triple-resonance four-dimensional NMR spectroscopy of a 46 ns tumbling protein** J. Am. Chem. Soc., 121 (1999), pp. 2571-2575

Zhang et al. 1994 O. Zhang, L.E. Kay, J.P. Olivier, J. Forman-Kay **Backbone 1H and 15N resonance assignments of N-terminal SH3 domain of drk in folded and unfolded states using enhanced-sensitivity pulsed field gradient NMR techniques** J. Biomol. NMR, 4 (1994), pp. 845-858